Translational Oncology
www.transonc.com

Volume 2 Number 1 March 2009 pp. 8–20 8

$\alpha_5\beta_1$ Integrin Ligand PHSRN Induces Invasion and α_5 mRNA in Endothelial Cells to Stimulate Angiogenesis[1]

Zhao-Zhu Zeng, Hongren Yao, Evan D. Staszewski, Korrene F. Rockwood, Sonja M. Markwart, Kevin S. Fay, Aaron C. Spalding[2] and Donna L. Livant

Department of Radiation Oncology and Comprehensive Cancer Center, University of Michigan, Ann Arbor, MI 48109-5637, USA

Abstract

Angiogenesis requires endothelial cell invasion and is crucial for wound healing and for tumor growth and metastasis. Invasion of native collagen is mediated by the $\alpha_5\beta_1$ integrin fibronectin receptor. Thus, $\alpha_5\beta_1$ up-regulation on the surfaces of endothelial cells may induce endothelial cell invasion to stimulate angiogenesis. We report that the interaction of $\alpha_5\beta_1$ with its PHSRN peptide ligand induces human microvascular endothelial cell invasion and that PHSRN-induced endothelial cell invasion is regulated by $\alpha_4\beta_1$ integrin and requires matrix metalloproteinase 1 (MMP-1). Moreover, our results show that exposure to PHSRN causes rapid, specific up-regulation of surface levels of $\alpha_5\beta_1$ integrin and significantly increases α_5 integrin mRNA in microvascular endothelial cells. Consistent with these results, α_5 small interfering RNA abrogates PHSRN-induced surface α_5 and MMP-1 up-regulation, as well as blocking invasion induction. We also observed dose-dependent, PHSRN-induced $\alpha_5\beta_1$ integrin up-regulation on endothelial cells *in vivo* in Matrigel plugs. We further report that the PHSCN peptide, an $\alpha_5\beta_1$-targeted invasion inhibitor, blocks PHSRN-induced invasion, $\alpha_5\beta_1$ up-regulation, α_5 mRNA induction, and MMP-1 secretion in microvascular endothelial cells and that systemic PHSCN administration prevents PHSRN-induced $\alpha_5\beta_1$ up-regulation and angiogenesis in Matrigel plugs. These results demonstrate a critical role for $\alpha_5\beta_1$ integrin and MMP-1 in mediating the endothelial cell invasion and angiogenesis and suggest that PHSRN-induced α_5 transcription and $\alpha_5\beta_1$ up-regulation may form an important feed-forward mechanism for stimulating angiogenesis.

Translational Oncology (2009) 2, 8–20

Introduction

Endothelial cells invade the extracellular matrix (ECM) early in angiogenesis. The $\alpha_5\beta_1$ and $\alpha_4\beta_1$ integrin fibronectin receptors (FnRs) of epithelial cells and fibroblasts have been shown to regulate invasion in response to plasma fibronectin (pFn), a significant component of all body fluids, and to pFn fragments made during wound healing [1,2]. The $\alpha_5\beta_1$ FnR specifically interacts with the PHSRN sequence of pFn cell binding domain (CBD) fragments to stimulate invasion [1,2], whereas the interaction of the $\alpha_4\beta_1$ FnR with the connecting segment LDV sequence functions to repress $\alpha_5\beta_1$-mediated invasion induction by intact pFn [3,4]. Because endothelial cells, fibroblasts, and epithelial cells express both $\alpha_4\beta_1$ and $\alpha_5\beta_1$ [2,5], invasion induction requires separation of their binding sites by pFn fragmentation, which occurs during clot dissolution [6].

The $\alpha_5\beta_1$ FnR is upregulated in late-stage tumors during establishment of the invasive phenotype [7], whereas $\alpha_4\beta_1$ may be downregulated to cause constitutive, Fn-dependent invasion [1,3,4]. In the absence of $\alpha_4\beta_1$/LDV binding, the $\alpha_5\beta_1$/PHSRN interaction stimulates matrix metalloproteinase 1 (MMP-1)–dependent invasion by both normal and metastatic carcinoma cells [1,3,4]. The importance of $\alpha_5\beta_1$-mediated invasion in malignant progression is suggested by results of both preclinical and clinical studies using an $\alpha_5\beta_1$ integrin–directed invasion inhibitor, the acetylated, amidated PHSCN peptide (Ac-PHSCN-NH_2 or ATN-161) to reduce tumorigenesis, block metastasis, and prevent progression [1,8–11].

Address all correspondence to: Donna L. Livant, Department of Radiation Oncology, University of Michigan, Room 4424F Medical Science 1, 1301 Catherine Street, Ann Arbor, MI 48109-5637. E-mail: dlivant@umich.edu

[1]This work was supported by a grant from Attenuon. The authors have no conflicting financial interests.

[2]Current address: St Jude Children's Research Hospital, 332 N. Lauderdale Street, Memphis, TN 38105.

Received 5 September 2008; Revised 7 October 2008; Accepted 8 October 2008

DOI 10.1593/tlo.08187

The $\alpha_5\beta_1$ fibronectin receptors of endothelial cells are important therapeutic targets for promoting wound healing or for inhibiting tumor growth and metastasis. $\alpha_5\beta_1$ Expression on endothelial cells is upregulated after the addition of angiogenic growth factors, especially during migration or angiogenic sprouting [12,13]. $\alpha_5\beta_1$ Expression is also increased on vascular endothelial cells during choroidal neovascularization [14], as well as on angiogenic sprouts in the central nervous system [15]. Moreover, $\alpha_5\beta_1$ integrin is uniformly overexpressed on the luminal surfaces of tumor blood vessels, whereas there is much reduced expression on quiescent endothelial cells [16,17]. These results suggest that invasion induction may specifically involve surface $\alpha_5\beta_1$ up-regulation, implying that in addition to stimulating invasion, the PHSRN/$\alpha_5\beta_1$ interaction may upregulate surface $\alpha_5\beta_1$ integrin levels, perhaps in part by inducing the mRNA encoding the α_5 integrin subunit in microvascular endothelial cells.

On the basis of these observations, we formulated the hypothesis that PHSRN induces $\alpha_5\beta_1$-mediated invasion by endothelial cells to promote angiogenesis. To test our hypothesis, we determined the effects of acetylated, amidated PHSRN peptide (Ac-PHSRN-NH_2) treatment on invasive behavior, on surface levels of $\alpha_5\beta_1$ FnR, and on α_5 mRNA levels in human microvascular endothelial cells (HMVECs). We also assayed the effects of Ac-PHSCN-NH_2, an $\alpha_5\beta_1$-targeted invasion inhibitor that prevented metastatic disease progression for prolonged periods in preclinical models and phase 1 clinical trial [1,8–11], on PHSRN-induced HMVEC invasion and on PHSRN-induced angiogenesis in Matrigel plugs in nude mice. We found that the PHSRN peptide induces MMP-1–dependent HMVEC invasion, upregulates surface $\alpha_5\beta_1$ integrin levels on HMVEC, in part by inducing α_5 integrin mRNA, and stimulates angiogenesis *in vivo*. Consistent with these results, we observed that both PHSRN-induced $\alpha_5\beta_1$ up-regulation and invasion were blocked in α_5-silenced HMVEC. We also report that the PHSCN peptide is a potent inhibitor of PHSRN-induced invasion, $\alpha_5\beta_1$ up-regulation, and angiogenesis.

Materials and Methods

Cell Culture, Peptide Synthesis, Invasion and MMP-1 Activity Assays, and Statistics

Dermal HMVECs (Clonetics, San Diego, CA) were cultured in MCDB131 medium (Mediatech, Inc., Herndon, VA) as recommended. pFn-Depleted FBS (Cambrex, Walkersville, MD) was prepared as described [1,3]. Naturally serum-free sea urchin embryo basement membranes (SU-ECM) were prepared for use as invasion substrates, and *in vitro* invasion assays were performed as described [1–4,18]. Acetylated, amidated PHSRN, HSPNR, LHGPEILDVPST (LDV), PGVLSEHPTLID (scrambled LDV), GRGDSP (RGD), VKNEED, PHSCN, and HSPNC peptides were synthesized as previously described [1–4]. In subsequent *in vitro* assays, serum-starved HMVECs were treated with the following combinations of peptides: 1 μg of Ac-PHSRN-NH_2 per 20,000 cells and/or equimolar concentrations of acetylated, amidated HSPNR, LDV, scrambled LDV, PHSCN, or HSPNC peptides. P1D6 anti-$\alpha_5\beta_1$, P1B5 anti-$\alpha_3\beta_1$, P4C2 anti-$\alpha_4\beta_1$, COMY4A2 anti–MMP-1, CA-4001 anti–MMP-2, or GE-213 anti–MMP-9 monoclonal antibody (mAb; Chemicon International, Temecula, CA), the 120-kDa Fn CBD (Chemicon), or isotype controls (Sigma-Aldrich, St. Louis, MO and eBioscience, San Diego, CA) were prebound to cells for invasion assays as described [1,3,4]. Adherent HMVECs were treated with peptides and MMP-1 activities determined as described [3,4]. MMP-1 activity was measured using the human active MMP-1 fluorescent assay system (R&D Systems, Minneapolis, MN). The relative fluorescence units of each well were determined with a SpectraMax MS plate reader (Molecular Devices, Sunnyvale, CA).

Plasma membranes, excluding organelles, were prepared from serum-starved, peptide-treated HMVEC as described above, according to [19,20]. Plasma membrane protein concentration was measured using the DC protein assay (Bio-Rad, Hercules, CA). Anti-α_5 mAb CD 49e (BD Biosciences, San Jose, CA) was used to analyze α_5 integrin expression by Western blot analysis. Anti-α_4 mAb P4C2 (Chemicon) was used to immunoprecipitate $\alpha_4\beta_1$ from plasma membrane extracts, and anti-β_1 mAb N29 (Chemicon) antibodies were used to analyze $\alpha_4\beta_1$ expression levels by Western blot analysis. Band densities were quantitated with ImageJ, obtained at http://rsb.info.nih.gov/ij/. *P* values were calculated with independent samples Student's *t* test statistical program SPSS 15.0 (SPSS, Inc., Chicago, IL).

Fluorescent Antibody Staining and Image Analysis of Fluorescence Intensity

Cells were serum-starved overnight on eight-well Permanox Lab-Tek Chamber slides before incubating with peptides as described above and/or with 1 mg/ml actinomycin D (Sigma) in 10% FBS for 2 hours at 37°C. Treated cells were rinsed, fixed, and blocked with normal goat serum (Vector Laboratories, Burlingame, CA) as previously described [21]. Treated cells were incubated overnight at 4°C in a mixture of anti-integrin and anti–MMP-1 primary antibodies: P1D6 anti-$\alpha_5\beta_1$ (mAb1969) or P4C2 anti-$\alpha_4\beta_1$ (mAb 1955) diluted 1:500, and rabbit anti–MMP-1 antiserum (Ab), diluted 1:400 (Chemicon), or with rabbit anti-$\alpha_5\beta_1$ Ab (AB1928) diluted 1:500 (Chemicon), in 5% normal goat serum in PBS and Triton overnight at 4°C. After rinsing, cells were incubated in antirabbit and antimouse secondary antibodies, conjugated with Cy3 or FITC, respectively (Jackson ImmunoResearch Laboratories, Inc., West Grove, PA). After rinsing, slides were mounted and analyzed by confocal microscopy as previously described [21–23]. The relative fluorescence intensities of $\alpha_5\beta_1$ and MMP-1 staining were calculated by using Image-Pro Plus software (Media Cybernetics, Inc., Silver Spring, MD). Exactly 20 isolated cells per treatment were selected randomly for analysis at 400-fold magnification by blindly choosing fields and analyzing all isolated cells in each field selected. The mean values of signal intensities were obtained from all chosen cells and then copied and pasted into Microsoft Excel data sheets for further analysis. All data are expressed as mean ± SD and evaluated with Student's *t* test (SPSS, Inc.). Significance was set at $P < .05$.

Real-time Reverse Transcription–Polymerase Chain Reaction

Confluent HMVECs were serum-starved and treated with peptides as described above. Total RNA was isolated using RNeasy Plus Mini Kit (QIAGEN GmbH, Hilden, Germany). RNA integrity was assessed with Agilent 2100 BioAnalyser (Agilent Technologies, Waldbronn, Germany). One-step reverse transcription–polymerase chain reaction (RT-PCR) was performed using the QIAGEN RT-PCR Kit (QIAGEN Catalog number 204243), as directed. The integrin α_5 primers used and reaction conditions have been previously described [24,25]. Glyceraldehyde 3-phosphate dehydrogenase primers were used as standards, as previously described [26]. Data were collected using ABI PRISM 7900HT Sequence Detection System (Applied Biosystems, Foster City, CA). Data analysis was performed with software SDS 2.2.1 (Applied

Biosystems). Normalized expression was calculated using the comparative threshold cycle (C_t) method, and fold changes were derived from the $2^{-\Delta\Delta Ct}$ values for α_5. α_5 Expression levels were normalized to glyceraldehyde 3-phosphate dehydrogenase as described [26]. *P* values were calculated with Student's *t* test statistical program SPSS 15.0 (SPSS, Inc.).

Integrin Subunit α_5 Small Interfering RNA Treatments

The integrin subunit α_5 small interfering RNA (siRNA), nonspecific control siRNA [27,28], fluorescein-conjugated control siRNA, siRNA transfection reagent, and siRNA transfection medium (catalog numbers sc-29372, sc-37007, sc-36869, sc-29528, and sc-36868, respectively) were purchased from Santa Cruz Biotechnology, Inc. (Santa Cruz, CA). Cells were seeded into six-well plates (2.5×10^5/well) in MCDB131 with 10% FBS 24 hours before transfection. Cells were transfected using siRNA transfection reagent (Santa Cruz Biotechnology) according to the manufacturer's instructions. The final concentration of siRNA in each well was 40 nM. At 72 hours after transfection, cells were harvested for invasion assays and fluorescent antibody staining. Fluorescein-conjugated control siRNA was used to evaluate transfection efficiency.

Matrigel Plug Assays

Matrigel plug assays were performed in female nude mice (Harlan Sprague Dawley, Inc., Indianapolis, IN) using protocols approved by the University Committee on Use and Care of Animals, as previously described [29–31]. Acetylated, amidated PHSRN (0.1, 0.5, or 2.5 mg) or HSPNR (2.5 mg) peptides, or 400 μg of basic fibroblast growth factor (bFGF; Fitzgerald Industries International, Inc., Concord, MA) were added to 0.5 ml of Matrigel before subcutaneous injection. Normal saline (NS), 0.1 ml containing 0.3 mg of acetylated, amidated PHSCN or HSPNC, was injected into tail veins (days 0, 2, and 4). Each treatment group consisted of 10 plugs in five mice. Plugs were removed (day 5), rinsed, and fixed as described [21–23]. Plugs were cryoprotected with a sucrose series of 5% to 20% and frozen in a mixture of Tissue-Tek OCT embedding medium [22]. Sections, 5 μm in thickness, were cut with a cryostat [21–23] from all plugs, mounted on slides, and stained using the HT15-IKT kit (Sigma), as directed. Mean numbers of microvessels were determined by counting 30 randomly chosen fields, at 400-fold magnification, on a microscope (Axioplan; Carl Zeiss, Inc., Thornwood, NY).

Drabkin's Assays for Hemoglobin

Matrigel plugs, each with 2.5 mg of PHSRN peptide or 2 million MATLyLu rat prostate cancer cells [30], were implanted in nude mice. Mice were treated with acetylated, amidated PHSCN or HSPNC peptides for a total of 9 (MATLyLu) or 16 (PHSRN) days, as described above. Plugs were removed and homogenized in 500 μl of PBS, and exactly one third of each homogenized plug was processed for hemoglobin levels, using Drabkin's reagent (Sigma), as directed. Each sample was assayed in duplicate, and results were normalized to plug protein concentrations using Spectra Max Plus 384 (Molecular Devices, Sunnyvale, CA). Experiments were repeated, and results were analyzed as described above.

Results

Endothelial Cell Invasion Regulated by $\alpha_5\beta_1$ and $\alpha_4\beta_1$ FnR and Their Peptide Ligands

Submicromolar PHSRN peptide concentrations were evaluated for HMVEC invasion induction using SU-ECM as invasion substrates in medium containing 10% FBS [1–4,18]. The scrambled sequence control, HSPNR, was also evaluated. In addition to the PHSRN sequence from the ninth type III module of the Fn CBD, $\alpha_5\beta_1$ binds the RGD and VKNEED sites reviewed in Altroff et al. [32]. Thus, the GRGDSP and VKNEED peptides (Ac-GRGDSP-NH_2 and Ac-VKNEED-NH_2) were also tested for HMVEC invasion induction. A peptide containing the $\alpha_4\beta_1$ binding site in the Fn type III connecting segment, the LDV peptide (Ac-LHGPEILDVPST-NH_2) and its scrambled sequence control, the scrambled LDV peptide (Ac-PGVLSEHPTLID-NH_2), were also combined with PHSRN at equimolar concentrations [33,34] and tested for repression of PHSRN-induced HMVEC invasion. As shown in Figure 1*A*, PHSRN stimulated HMVEC invasion with a log-linear dose-response relationship at concentrations from 17 nM to 1.7 μM (10 ng/ml to 1 μg/ml), whereas HSPNR had no activity. Neither RGD nor VKNEED induced HMVEC invasion at concentrations of 1.7 μM (1.0 μg/ml). Figure 1*A* also shows that the presence of equimolar LDV peptide prevented PHSRN-induced HMVEC invasion, whereas an identical concentration of scrambled LDV had no inhibitory effect. Also, neither LDV nor scrambled LDV alone induced HMVEC invasion (data not shown). These results are consistent with the invasive responses to PHSRN and HSPNR peptides observed for mammary epithelial cells, normal keratinocytes, fibroblasts, and prostate epithelial cells in the presence of FBS and for metastatic human breast and prostate cancer cell lines on serum-free SU-ECM substrates [1–4,11]. As expected from the presence of both the PHSRN and LDV sequences on intact fibronectin, no invasion was observed in the presence of 10% FBS without added PHSRN. Thus, the ability of LDV to inhibit PHSRN-induced HMVEC invasion is consistent with the expression of $\alpha_5\beta_1$ and $\alpha_4\beta_1$ FnR on endothelial cells [5,35].

The role of $\alpha_5\beta_1$ integrin in PHSRN-induced HMVEC invasion was confirmed through the use of the blocking anti-$\alpha_5\beta_1$ mAb, P1D6 [36]. The effects of increasing concentrations of P1D6 on PHSRN-induced HMVEC invasion are shown in Figure 1*B*: the mean invasion percentages of HMVECs pretreated with P1D6, before placement of SU-ECM in the presence of 1 μg/ml PHSRN peptide in 10% FBS, are plotted. Invasion declined log-linearly, with respect to increasing P1D6 concentrations, whereas prebinding the cells to elevated concentrations of P1B5 blocking anti-α_3 mAb had no effect.

Because the $\alpha_4\beta_1$/LDV interaction represses $\alpha_5\beta_1$-mediated invasion and MMP-1 induction [3,4,37], the effects of blocking anti-$\alpha_4\beta_1$ mAb (P4C2) on HMVEC invasion were assessed. Suspended HMVECs were prebound to increasing concentrations of P4C2, then placed on SU-ECM in 10% FBS. The effects of P4C2 on HMVEC invasion are shown in Figure 1*C*: the mean invasion percentages of P4C2-treated HMVECs, relative to a positive control (1.0 μg/ml PHSRN), are plotted. Invasion increased log-linearly with increasing P4C2 concentration, whereas the isotype control had no effect. The dependence of P4C2 anti–$\alpha_4\beta_1$-induced HMVEC invasion on pFn was also confirmed. As shown in Figure 1*D*, no P4C2-induced invasion occurred in 10% pFn-depleted FBS [1], whereas addition of purified pFn, at the concentration found in 10% FBS, seemed to fully restore P4C2-induced invasion. These results illustrate the dependence of invasion on fibronectin.

Role of MMP-1 in $\alpha_5\beta_1$-Mediated HMVEC Invasion

The importance of MMP-1 collagenase in angiogenesis *in vitro* [38] and the induction of MMP-1 secretion and MMP-1–dependent

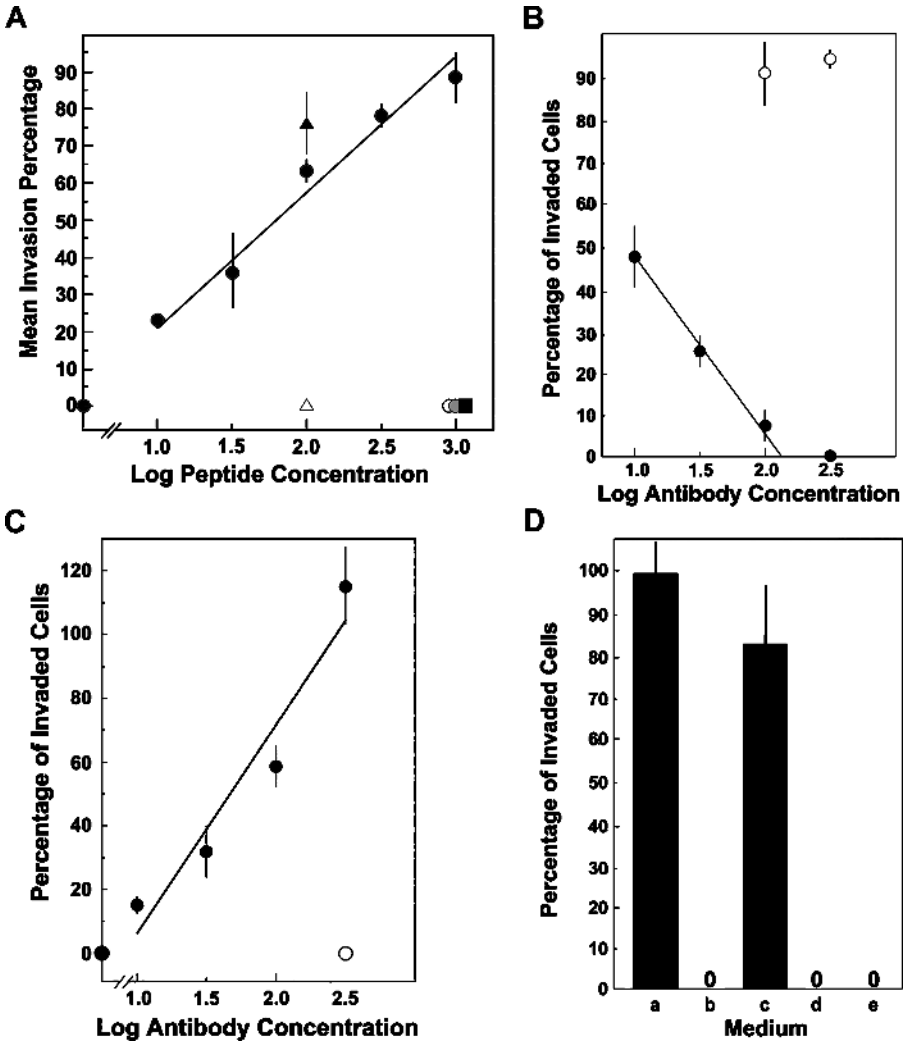

Figure 1. Invasion regulation by PHSRN and LHGPEILDVPST. (A) PHSRN-induced invasion. *X*-axis, log peptide concentration (ng/ml); *Y*-axis, mean invasion percentages relative to maximally stimulated controls (±SD). Black circles, 10 ng/ml to 1 μg/ml Ac-PHSRN-NH_2. Controls: black square, 1 μg/ml Ac-HSPNR-NH_2; white circle, 1.0 μg/ml Ac-GRGDSP-NH_2; gray circle, 1.0 μg/ml Ac-VKNEED-NH_2; white triangle, 100 ng/ml Ac-PHSRN-NH_2 + 250 ng/ml Ac-LHGPEILDVPST-NH_2; black triangle, 100 ng/ml Ac-PHSRN-NH_2 + 250 ng/ml Ac-PGVLSEHPTLID-NH_2. (B) Inhibition of PHSRN-induced invasion by P1D6 anti-$\alpha_5\beta_1$ mAb. *X*-axis, log Ab concentration (μg/ml); *Y*-axis, mean invasion percentages, relative to 1 μg/ml Ac-PHSRN-NH_2 without added P1D6 (±SD). Black circles, 10 to 300 μg/ml P1D6 mAb in the presence of 1.0 μg/ml Ac-PHSRN-NH_2. White circles, 100 or 300 μg/ml P1B5 anti-$\alpha_3\beta_1$ mAb in the presence of 1.0 μg/ml Ac-PHSRN-NH_2. (C) Invasion induction by anti-$\alpha_4\beta_1$ blocking mAb P4C2. *X*-axis, log micrograms of P4C2 mAb per milliliter; *Y*-axis, mean percentages of invaded cells relative to 1 μg/ml Ac-PHSRN-NH_2 (±SD). Black circles, 0 to 300 μg/ml P4C2; white circle, 300 μg/ml isotype control. (D) Dependence of P4C2-induced invasion on the presence of pFn. *X*-axis, media: a, 10% FBS with 300 μg/ml P4C2; b, 10% pFn-depleted FBS with 300 μg/ml P4C2; c, 10% pFn-depleted FBS, with 10 μg/ml pFn and 300 μg/ml P4C2; d, 10% pFn-depleted FBS, with 10 μg/ml pFn and 300 μg/ml isotype control Ab; e, 10% FBS, with 300 μg/ml isotype control. *Y*-axis, mean percentages of invaded cells relative to 1 μg/ml Ac-PHSRN-NH_2 (±SD).

invasion by the PHSRN/$\alpha_5\beta_1$ interaction [3,4] suggested that $\alpha_5\beta_1$-mediated HMVEC invasion specifically requires MMP-1 and that the PHSRN peptide stimulates MMP-1 secretion. These hypotheses were tested by prebinding HMVEC to increasing concentrations of blocking COMY4A2 anti–MMP-1 mAb, then inducing $\alpha_5\beta_1$-mediated HMVEC invasion in each of two ways: 1) treatment with 100 ng/ml PHSRN peptide or 2) binding to 300 μg/ml P4C2 blocking anti-$\alpha_4\beta_1$ mAb. Treated cells were placed on SU-ECM to quantitate invasion. As shown in Figure 2*A*, prebinding HMVEC to increasing concentrations of COMY4A2 caused a log-linear decline in PHSRN-induced invasion, whereas prebinding to blocking anti–MMP-2 or anti–MMP-9 mAb had no effect. Similarly, as shown in Figure 2*B*, increasing concentrations of COMY4A2 inhibited P4C2-induced HMVEC invasion, whereas neither anti–MMP-2 nor anti–MMP-9 had discernable effects.

The effects of PHSRN and LDV on MMP-1 secretion were assessed by spectrophotometric activity assays, performed on the concentrated medium of adherent HMVEC, treated with combinations of PHSRN, LDV, and scrambled LDV peptides. Exposure to PHSRN stimulated the secretion of activated MMP-1, relative to untreated controls, as shown in Figure 2*C*. Also, PHSRN-induced MMP-1 secretion was prevented by the inclusion of equimolar LDV. In contrast, inclusion

of equimolar scrambled LDV sequence peptide had no significant effect on PHSRN-induced MMP-1. These results are consistent with those obtained for normal human mammary and prostate epithelial cells [3,4].

Inhibition of $\alpha_5\beta_1$-Mediated Invasion and MMP-1 Secretion by PHSCN

The PHSCN peptide has been shown to have significant antitumorigenic and antimetastatic activities *in vivo* [1,9–11]. Because angiogenesis is important for both tumorigenesis and metastasis, PHSCN was evaluated for its ability to block $\alpha_5\beta_1$-mediated invasion and MMP-1 secretion by HMVEC. To evaluate the anti-invasive activity of PHSCN, HMVECs were treated with Ac-PHSCN-NH_2 at 1.7 μM (1.0 μg/ml) and were placed on SU-ECM in the presence of 3.0 μg/ml 120-kDa pFn CBD to elicit $\alpha_5\beta_1$-mediated invasion. As shown in Figure 3*A*, PHSCN prevented CBD-induced HMVEC invasion, whereas an equal concentration of the scrambled PHSCN sequence control had no effect. To assess the effects of PHSCN on FBS-induced invasion, HMVECs were pretreated with 300 μg/ml P4C2 then bound to 1.7 μM (1.0 μg/ml) PHSCN or HSPNC peptides and placed on SU-ECM in 10% FBS. As shown in Figure 3*B*, exposing the cells to PHSCN prevented P4C2-induced invasion, whereas equal concentrations of HSPNC had no effect. The dose-response relationship of PHSCN on PHSRN-induced invasion of SU-ECM by HMVEC was determined, and the results are shown in Figure 3*C*: HMVEC invasion was induced by 170 nM (100 ng/ml Ac-PHSRN-NH_2) and was inhibited with 17 nM to 1.7 μM (10 ng/ml to 1.0 μg/ml) Ac-PHSCN-NH_2. PHSRN-induced HMVEC invasion declined log-linearly with increasing PHSCN peptide concentration and was prevented at the highest concentrations. The scrambled PHSCN sequence control, 1.7 μM (1.0 μg/ml) Ac-HSPNC-NH_2, had no inhibitory effect. Analogous effects of PHSCN on PHSRN-induced MMP-1 secretion by HMVEC were also observed in MMP-1 activity assays, as shown in Figure 3*D*. The PHSRN peptide induced dose-dependent MMP-1 secretion, and HSPNR had no effect. The presence of equimolar PHSCN peptide reduced PHSRN-induced MMP-1 secretion to background levels, whereas equimolar HSPNC peptide was not inhibitory.

Regulation of Cell Surface $\alpha_5\beta_1$ Integrin Levels in HMVEC by PHSRN and PHSCN Peptides

Because higher levels of $\alpha_5\beta_1$ receptors are observed on the surfaces of endothelial cells in angiogenic sprouts [12–14], $\alpha_5\beta_1$-mediated, PHSRN-induced HMVEC invasion may involve the up-regulation of surface $\alpha_5\beta_1$, as well as MMP-1 secretion. Hence, the effects of the PHSRN peptide on surface $\alpha_5\beta_1$ and MMP-1 were assessed by fluorescent antibody staining. Adherent HMVECs were treated for 2 hours with 0.5 μg/ml Ac-PHSRN-NH_2 in FBS-containing medium. Then, the PHSRN-treated HMVECs were fixed, and bound to fluorescein-tagged anti-α_5 integrin and rhodamine-tagged anti–MMP-1 Ab. To visualize the locations of their nuclei, the cells were also bound to 4′,6′-diamidino-2-phenylindole (DAPI). Similar experiments were also performed with fluorescein-tagged P1D6 anti-$\alpha_5\beta_1$ mAb. Immunofluorescence was quantitatively analyzed by confocal microscopy, and the results are shown in Figure 4. Figure 4*A* shows typical examples of anti-α_5 Ab- and anti–MMP-1 Ab-stained and DAPI-stained adherent HMVEC, after treatment with acetylated, amidated PHSRN, HSPNR, PHSRN and LDV, PHSRN and scrambled LDV, PHSRN and PHSCN, or PHSRN and HSPNC peptides.

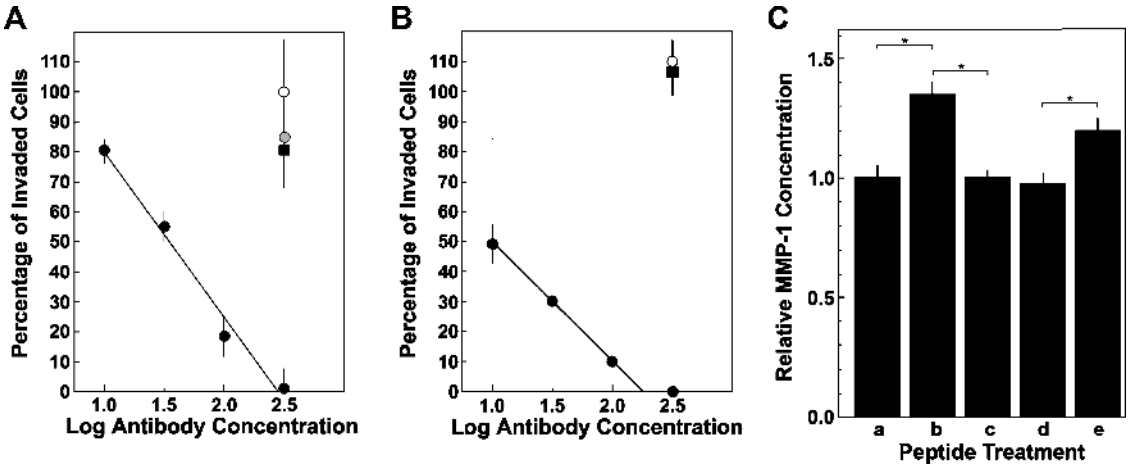

Figure 2. Inhibition of $\alpha_5\beta_1$-mediated invasion by COMY4A2 anti–MMP-1, and regulation of MMP-1 secretion by FnR peptide ligands. (A) Inhibition of PHSRN-induced invasion by COMY4A2 anti–MMP-1 mAb. *X*-axis, log micrograms of COMY4A2 mAb per milliliter; *Y*-axis, mean percentages of invaded microvascular cells (±SD), relative to 0.1 μg/ml Ac-PHSRN-NH_2, with no added mAb. All HMVEC induced by 0.1 μg/ml Ac-PHSRN-NH_2. Black circles, COMY4A2 anti–MMP-1; white circle, GE-213 anti–MMP-9; gray circle, CA-4001 anti–MMP-2; black square, COMY4A2 isotype control. (B) Inhibition of P4C2-induced invasion by COMY4A2 anti–MMP-1. *X*-axis, log micrograms of COMY4A2 mAb per milliliter; *Y*-axis, mean percentages of invaded microvascular cells (±SD), relative to HMVEC in 300 μg/ml P4C2 anti-$\alpha_4\beta_1$, without anti-MMP mAb. Black circles, increasing concentrations of COMY4A2 anti–MMP-1; black square, 300 μg/ml CA-4001 anti–MMP-2; white circle, 300 μg/ml GE-213 anti–MMP-9. (C) Effects of PHSRN and LDV peptides on MMP-1 secretion. *X*-axis, treatments: a, no added peptide; b, Ac-PHSRN-NH_2 (5 μg/5 ml per 20,000 cells); c, Ac-LHGPEILDVPST-NH_2 (12.5 μg/5 ml per 20,000 cells); d, equimolar Ac-PHSRN-NH_2 and Ac-LHGPEILDVPST-NH_2 (5 μg/5 ml per 20,000 cells and 12.5 μg/5 ml per 20,000 cells, respectively); e, equimolar Ac-PHSRN-NH_2 and Ac-PGVLSEHPTLID-NH_2 (5 μg/5 ml per 20,000 cells and 12.5 μg/5 ml per 20,000 cells, respectively). *Y*-axis, mean relative MMP-1 concentrations (±SD). *$P < .01$.

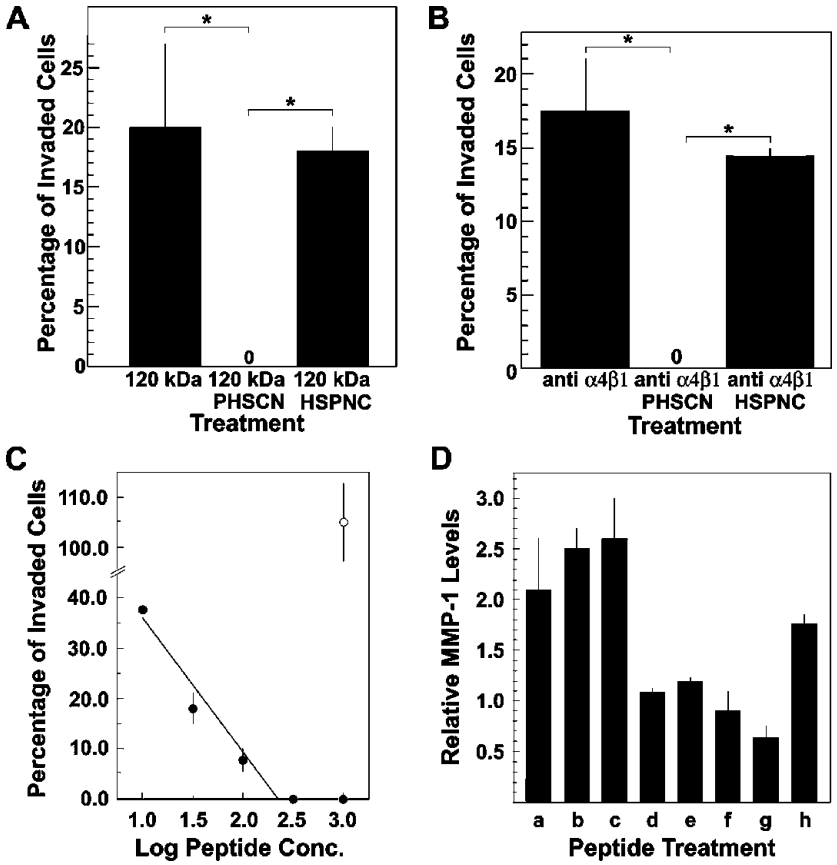

Figure 3. Inhibition of $\alpha_5\beta_1$-mediated invasion, and PHSRN-induced MMP-1 secretion by PHSCN. (A) Inhibition of CBD-induced HMVEC invasion by PHSCN. *X*-axis, HMVEC treatment: 120 kDa, 3 μg/ml 120-kDa pFn CBD; 120 kDa + PHSCN, 3 μg/ml 120-kDa pFn CBD + 1 μg/ml Ac-PHSCN-NH_2; 120 kDa + HSPNC, 3 μg/ml 120-kDa pFn CBD + 1 μg/ml Ac-HSPNC-NH_2. *Y*-axis, mean percentages of invaded cells (±SD). *$P < .01$. (B) Inhibition of P4C2 mAb-induced invasion by PHSCN. *X*-axis, HMVEC treatment: anti-$\alpha_4\beta_1$, 300 μg/ml P4C2; anti-$\alpha_4\beta_1$ + PHSCN, 300 μg/ml P4C2 + 1.0 μg/ml Ac-PHSCN-NH_2; anti-$\alpha_4\beta_1$ + HSPNC, 300 μg/ml P4C2 + 1.0 μg/ml Ac-HSPNC-NH_2. *Y*-axis, mean percentages of invaded cells (±SD). *$P < .01$. (C) Inhibition of PHSRN-induced invasion by PHSCN. *X*-axis, log nanograms of peptide concentrations per milliliter; *Y*-axis, mean percentages of invaded cells relative to 1.0 μg/ml Ac-PHSRN-NH_2 (±SD). Black circles, Ac-PHSCN-NH_2; white circle, Ac-HSPNC-NH_2. All samples contained 1.0 μg/ml Ac-PHSRN-NH_2. (D) Inhibition of PHSRN-induced MMP-1 secretion by PHSCN. *X*-axis, peptide treatment: a, 1 μg of Ac-PHSRN-NH_2/ml per 20,000 cells; b, 3 μg of Ac-PHSRN-NH_2/ml per 20,000 cells; c, 10 μg of Ac-PHSRN-NH_2/ml per 20,000 cells; d, 1 μg of Ac-HSPNR-NH_2/ml per 20,000 cells; e, 1 μg of Ac-PHSCN-NH_2/ml per 20,000 cells; f, 1 μg of Ac-HSPNC-NH_2/ml per 20,000 cells; g, Ac-PHSRN-NH_2 and Ac-PHSCN-NH_2, each 1 μg/ml per 20,000 cells; h, Ac-PHSRN-NH_2 and Ac-HSPNC-NH_2, each 1 μg/ml per 20,000 cells. *Y*-axis, mean MMP-1 concentrations relative to untreated controls: triplicate samples without added peptide (±SD).

PHSRN peptide treatment caused a rapid increase in anti-α_5 integrin Ab immunostaining, as well as a corresponding increase in anti–MMP-1 binding, whereas HSPNR peptide treatment had no effect, thus confirming the sequence specificity of PHSRN-induced α_5 and MMP-1 up-regulation. PHSRN-induced α_5 up-regulation was likely to result from the binding of PHSRN by the $\alpha_5\beta_1$ integrin because inclusion of an equimolar amount of the $\alpha_4\beta_1$ integrin fibronectin receptor LDV peptide ligand prevented both $\alpha_5\beta_1$ and MMP-1 up-regulation, whereas inclusion of equimolar scrambled LDV sequence peptide had no effect. PHSRN-induced α_5 and MMP-1 up-regulation could also be prevented by the inclusion of the transcription inhibitor, actinomycin D, suggesting that the observed changes in cell surface levels of $\alpha_5\beta_1$ and MMP-1 may involve changes in gene expression. Consistent with its ability to inhibit $\alpha_5\beta_1$-mediated, PHSRN-induced invasion, an equimolar concentration of the PHSCN peptide prevented PHSRN-induced surface α_5 integrin up-regulation, whereas the HSPNC scrambled sequence control had no effect. Identical results were obtained for all of these assays using fluorescein-tagged P1D6 anti-$\alpha_5\beta_1$ mAb (not shown). Figure 4*B* shows the quantitation of these effects on surface α_5 and $\alpha_5\beta_1$ levels (obtained with anti-α_5 Ab and with P1D6 anti-$\alpha_5\beta_1$ mAb) and MMP-1 levels (obtained with anti–MMP-1 Ab). PHSRN treatment increased mean anti-α_5 and $\alpha_5\beta_1$ fluorescence levels by three- to four-fold, respectively. PHSRN treatment also increased mean anti–MMP-1 fluorescence levels by four-fold. PHSRN induction of anti-α_5, anti-$\alpha_5\beta_1$, and anti–MMP-1 immunofluorescence was prevented by actinomycin D and by the LDV and PHSCN peptides. Scrambled sequence controls for the LDV and PHSCN peptides had no effect on PHSRN-induced up-regulation. The ability of the PHSRN peptide to induce invasion by surface $\alpha_5\beta_1$ up-regulation and the invasion-inhibitory function of $\alpha_4\beta_1$ suggest that PHSRN-treated HMVEC should not exhibit increased surface $\alpha_4\beta_1$. This was tested by comparing immunofluorescent staining of PHSRN- and HSPNR-treated HMVEC using the following primary antibodies: P4C2 anti-$\alpha_4\beta_1$ mAb, anti–MMP-1 Ab, P1D6 anti-$\alpha_5\beta_1$ mAb, and anti-α_5 Ab. As shown in Figure 4*C*, PHSRN treatment caused a significant up-regulation of surface $\alpha_5\beta_1$, as indicated by

P1D6 mAb and anti-α_5 Ab immunostaining, as well as MMP-1; but failed to induce increased surface $\alpha_4\beta_1$. These results were confirmed by immunoblot analysis as shown in the inset to Figure 4*C*. Immunoblots of extracts from membranes of PHSRN-treated HMVEC exhibited a 5.5-fold increase in CD 49e anti-α_5 mAb immunoreactivity, relative to untreated controls, whereas extracts from HSPNR-treated HMVEC showed no increase. Also, whereas membrane-bound α_5 integrin was increased by PHSRN treatment, the levels of β_1 integrin in P4C2 anti-α_4 immunoprecipitates remained unchanged. These results are both qualitatively and quantitatively similar to those obtained by immunofluorescence analysis (Figure 4*B*) and show that PHSRN specifically induces the up-regulation of membrane-bound, invasion-stimulatory $\alpha_5\beta_1$ without affecting levels of the invasion-inhibitory $\alpha_4\beta_1$ fibronectin receptor.

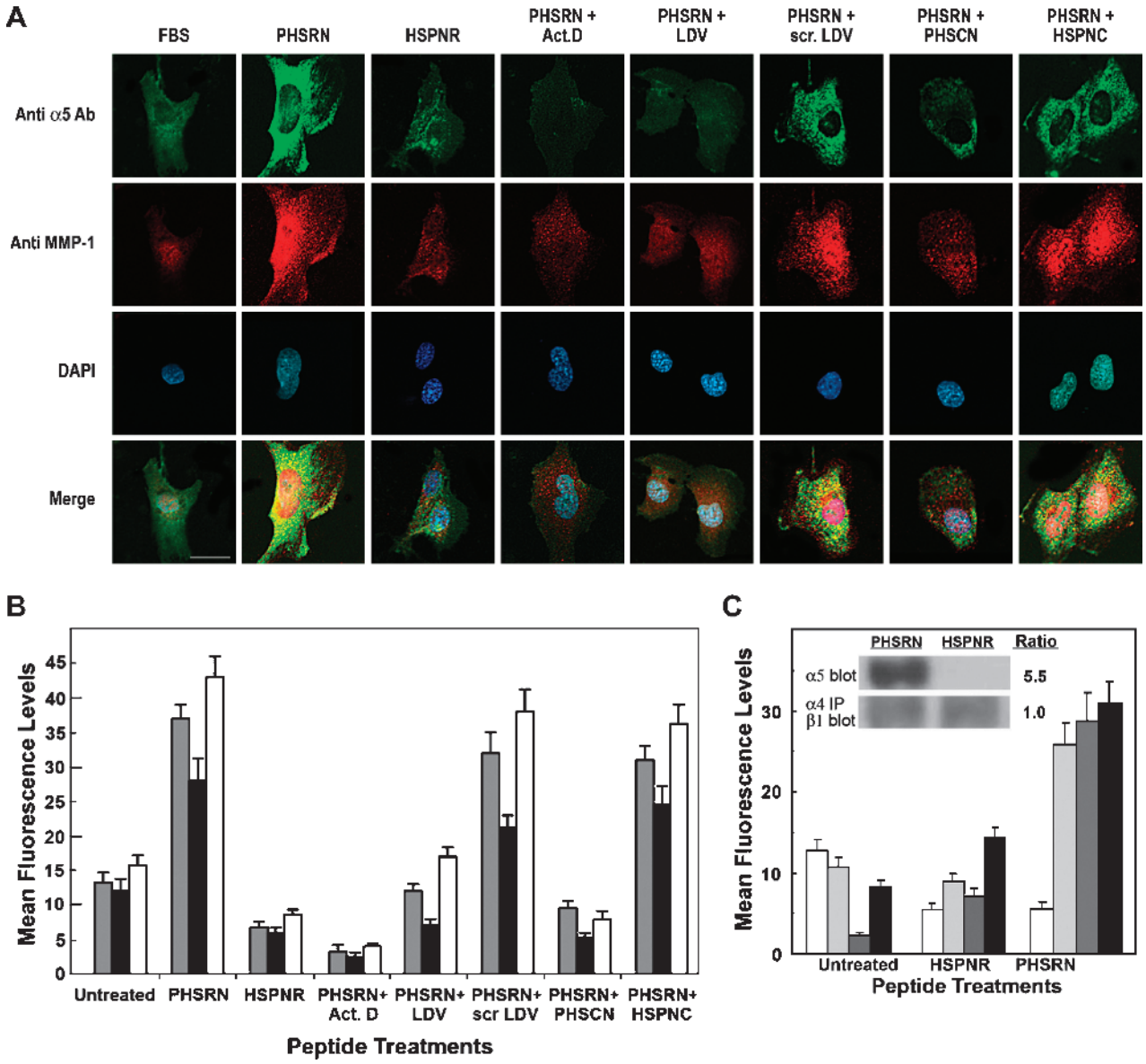

Figure 4. Up-regulation of $\alpha_5\beta_1$ and MMP-1 by PHSRN and inhibition by PHSCN. (A) HMVEC, stained with fluorescein-coupled anti-α_5 Ab, rhodamine-coupled anti–MMP-1 Ab, and DAPI. Peptide treatments and 5-μm bar are indicated. (B) Quantitation of fluorescence in HMVEC stained with fluorescein-coupled P1D6 anti-$\alpha_5\beta_1$ mAb or anti-α_5 Ab and rhodamine-coupled anti–MMP-1 Ab. *X*-axis, peptide treatments; *Y*-axis, mean fluorescence levels (±SD). PHSRN and HSPNR: 0.5 μg/ml; LDV and scrambled LDV: 1.5 μg/ml; PHSCN and HSPNC: 0.5 μg/ml. Act. D, actinomycin D; gray bars, P1D6 mAb; black bars, anti-α_5 Ab; white bars, anti–MMP-1 Ab. (C) Fluorescence quantitation in HMVEC stained with P4C2 anti-$\alpha_4\beta_1$, anti–MMP-1 Ab, P1D6 anti-$\alpha_5\beta_1$ mAb or anti-α_5 Ab. *X*-axis, peptide treatments; *Y*-axis, mean fluorescence (±SD). PHSRN and HSPNR as described above. White bars, P4C2 anti-$\alpha_4\beta_1$ mAb; light gray bars, anti–MMP-1 Ab; dark gray bars, P1D6 anti-$\alpha_5\beta_1$ mAb; black bars, anti-α_5 Ab. Inset: Effects of PHSRN or HSPNR on $\alpha_5\beta_1$ and $\alpha_4\beta_1$ levels in HMVEC plasma membranes. Anti-α_5 Ab immunoblot: mean (±SD) relative densities of α_5 bands from membrane extracts of PHSRN-treated HMVEC: 8.2 (±0.8); mean (±SD) relative densities of α_5 bands from HSPNR-treated HMVEC: 1.5 (±0.5). $P < .01$. Anti-β_1 immunoblots of anti-α_4 immunoprecipitates from membrane extracts of PHSRN- or HSPNR-treated HMVEC: mean (±SD) relative density of β_1 band from PHSRN-treated HMVEC: 1.1 (±0.1); mean (±SD) relative density of β_1 band from HSPNR-treated HMVEC: 1.1 (±0.0).

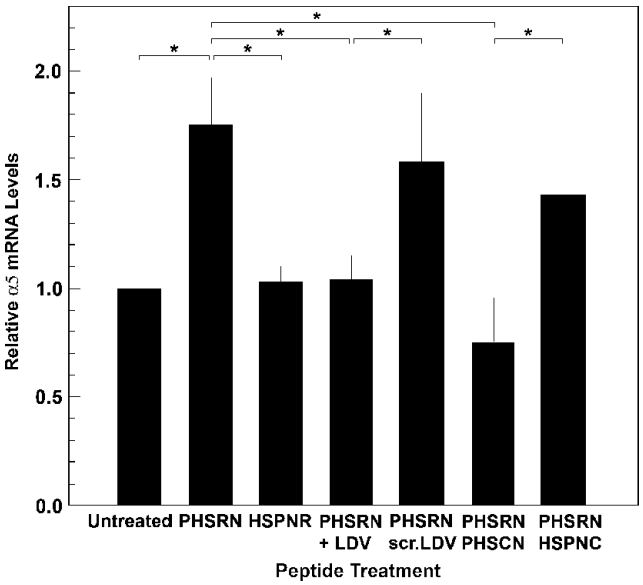

Figure 5. Induction of α_5 mRNA by the PHSRN/$\alpha_5\beta_1$ interaction. *X*-axis, peptide treatment: 1 μg/ml/20,000 cells PHSRN, HSPNR, PHSCN, or HSPNC peptides; 2.5 μg/ml/20,000 cells LDV or scr. LDV peptides: *Y*-axis, mean relative α_5 mRNA levels (±SD). *P* values for all starred comparisons: $P < .01$.

Regulation of α_5 Integrin mRNA Levels in HMVEC by PHSRN, LDV, and PHSCN Peptides

Inhibition of PHSRN-induced α_5 up-regulation by actinomycin D suggested that PHSRN may stimulate transcription of the gene encoding the α_5 integrin subunit. This was tested by treating adherent HMVEC with PHSRN or HSPNR peptides, and by ascertaining the effects of equimolar concentrations of the LDV and PHSCN peptides or their scrambled sequence controls, on PHSRN-induced α_5 mRNA levels by performing RT-PCR analysis. As shown in Figure 5, treatment of adherent HMVEC with PHSRN for 12 hours significantly increased α_5 mRNA levels, whereas treatment with HSPNR had no effect. Although the fold increase in surface $\alpha_5\beta_1$ in PHSRN-treated HMVEC, as determined by fluorescent antibody staining and by Western blot analysis (Figure 4), may be somewhat greater than the fold increase in α_5 mRNA, it has been previously reported that the quantitative correlation between mRNA and protein expression is often imperfect because of important posttranscriptional regulatory mechanisms [39]. As shown in Figure 5, equimolar LDV peptide prevented PHSRN-induced α_5 mRNA induction, whereas scrambled LDV peptide had no effect. On the basis of the known ability of the $\alpha_4\beta_1$/LDV interaction to inhibit PHSRN-induced invasion [3,4], as well as Fn CBD-induced MMP-1 transcription [37], these results suggest that the $\alpha_5\beta_1$/PHSRN interaction stimulates transcription of the α_5 integrin subunit gene. The results shown in Figure 5 also indicate that the presence of equimolar PHSCN peptide prevented PHSRN-induced α_5 mRNA induction in HMVEC, whereas the HSPNC scrambled sequence control had no effect.

Inhibition of PHSRN-Induced $\alpha_5\beta_1$ and MMP-1 Up-regulation and PHSRN-Induced Invasion by α_5 Integrin siRNA

The induction of α_5 mRNA by PHSRN peptide treatment suggested that transcription of the gene encoding the α_5 integrin subunit might be necessary for both surface $\alpha_5\beta_1$ up-regulation and $\alpha_5\beta_1$-mediated invasion in HMVEC. To evaluate the requirement for α_5 mRNA in PHSRN-induced surface $\alpha_5\beta_1$ up-regulation, adherent HMVECs transfected with α_5 or nonspecific control (NC) siRNA were treated with PHSRN peptide. Treated cells were stained with anti-$\alpha_5\beta_1$ and MMP-1 primary and fluorescent secondary antibodies and were analyzed by confocal microscopy. Mean fluorescence levels are shown in Figure 6*A* with their first SDs. Integrin α_5 siRNA inhibited the expression of α_5 subunit mRNA in adherent, fluorescent antibody–stained, PHSRN-treated HMVECs (images not shown). Irrespective of which siRNA was expressed, surface $\alpha_5\beta_1$ integrin and cytoplasmic MMP-1 levels differed only slightly in untreated HMVEC. However, PHSRN induction of both $\alpha_5\beta_1$ and MMP-1 declined

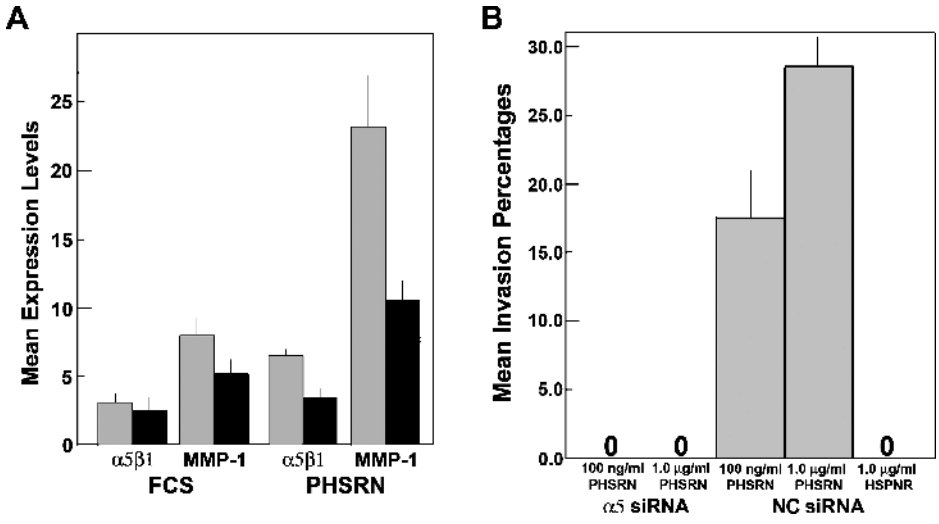

Figure 6. Inhibition of PHSRN-induced $\alpha_5\beta_1$ and MMP-1 up-regulation, and PHSRN-induced invasion by α_5 silencing. (A) Fluorescence quantitation of HMVEC, expressing either α_5 or nonspecific control (NC) siRNA. *X*-axis, treatments; black bars, α_5 siRNA; gray bars, NC siRNA; *Y*-axis, mean expression levels (±SD). (B) Effects of PHSRN peptide treatment on invasion by HMVEC expressing either α_5 or NC siRNA. *X*-axis, treatments; *Y*-axis, mean invasion percentages (±SD).

significantly in α_5 siRNA-expressing HMVEC, relative to those expressing NC siRNA. Consistent with these results, PHSRN-induced invasion was prevented in HMVEC expressing α_5 siRNA, whereas it was unaffected by the expression of NC siRNA, as shown in Figure 6*B*.

Inhibition of PHSRN-Induced Angiogenesis in Matrigel Plugs by Systemic PHSCN

PHSRN-induced, $\alpha_5\beta_1$-mediated angiogenesis was assessed in nude mice bearing Matrigel plugs [40,41]. Varying amounts of acetylated, amidated PHSRN, ranging from 0.1 to 2.5 mg, were included in Matrigel plugs, implanted subcutaneously. Plugs containing 2.5 mg of the HSPNR control were also included, as were plugs containing 400 ng of bFGF, a known proangiogenic agent [40]. After 5 days, plugs were removed and fixed; frozen sections were stained with Biebrich scarlet acid fuchsin and were counterstained with aniline blue. Neovascularization was quantitated by confocal microscopy. Each treatment group consisted of four to five nude mice, each bearing two plugs. As shown in Figure 7*A*, inclusion of PHSRN stimulated angiogenesis in a dose-dependent fashion, whereas inclusion of 2.5 mg of HSPNR had no effect. At the highest PHSRN dose, the mean numbers of microvessels observed were indistinguishable from the numbers observed in the bFGF-positive control.

Because the PHSCN peptide may bind purified $\alpha_5\beta_1$ integrin and has been reported to inhibit vascular endothelial growth factor– and bFGF-induced angiogenesis in Matrigel plugs [42], the antiangiogenic activity of systemic PHSCN was assessed in Matrigel plugs, each containing 0.5 mg of PHSRN to induce $\alpha_5\beta_1$-mediated angiogenesis, as above. While mice bore the plugs, they received three intravenous doses of PHSCN in NS; doses varied from 10 to 300 μg (0.5-15 mg/kg), the optimal systemic dose range for this agent [1,42]. Mice bearing plugs containing 0.5 mg of HSPNR were included as negative controls for PHSRN-induced angiogenesis; these mice received intravenous NS only. Also, mice bearing plugs containing 0.5 mg of PHSRN peptide were treated intravenously with 500 μg (25 mg/kg) of HSPNC as negative controls for systemic PHSCN therapy. Mice bearing plugs containing bFGF were also included, as above. After 5 days, all plugs were removed, fixed, sectioned, stained, and assayed as above. Increasing doses of intravenous PHSCN peptide inhibited PHSRN-induced angiogenesis in Matrigel plugs in a dose-dependent fashion, as shown in Figure 7*B*. Also, no angiogenesis inhibition was observed in HSPNC-treated mice. Figure 7*C* shows typical examples of the sections analyzed in these experiments: Matrigel only, Matrigel with 0.5 mg of PHSRN, and Matrigel with 0.5 mg of PHSRN, after a total of three intravenous doses of PHSCN (15 mg/kg).

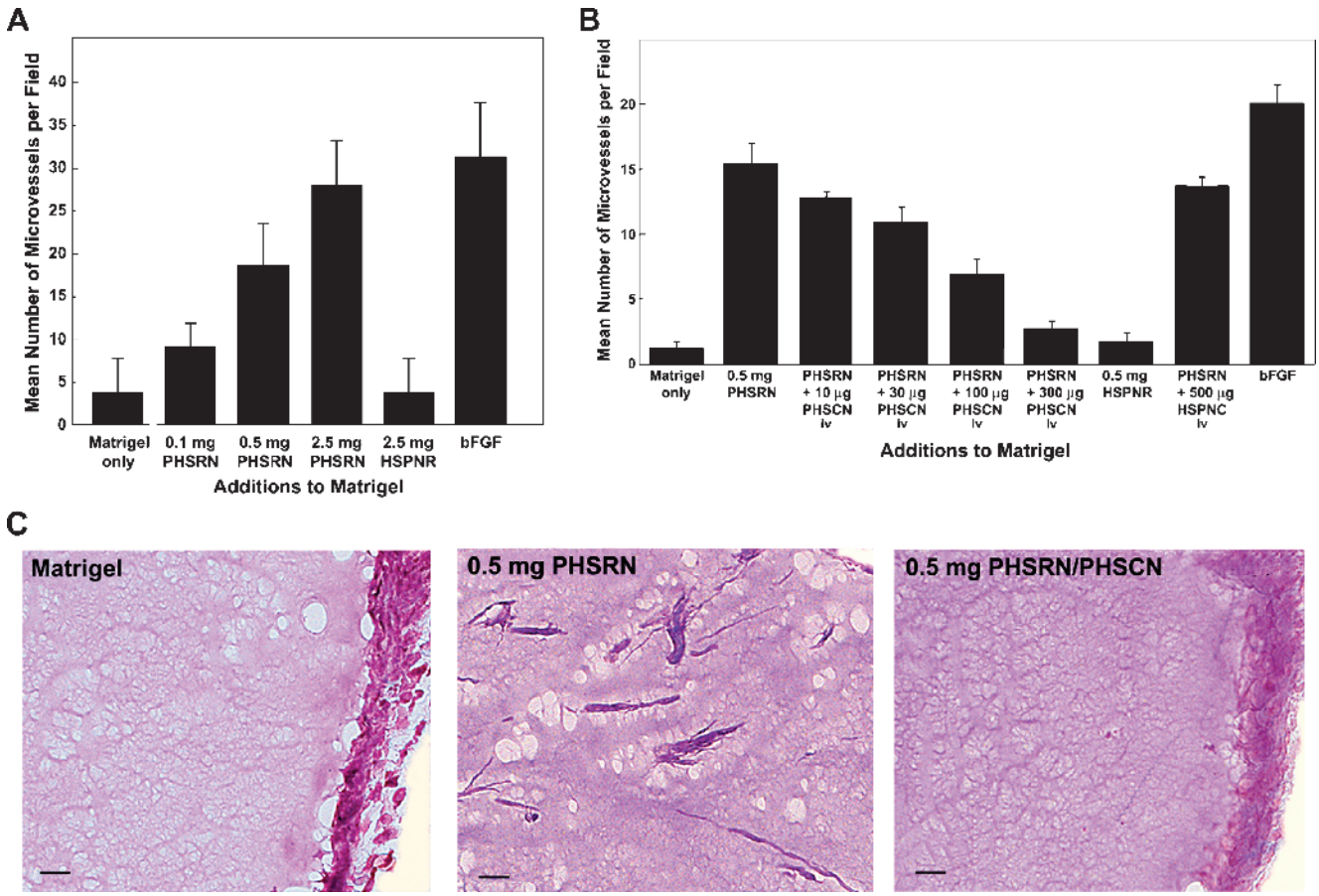

Figure 7. PHSCN inhibition of PHSRN peptide–induced angiogenesis in Matrigel plugs. (A) Angiogenesis induction by addition of PHSRN. *X*-axis, additions to Matrigel: PHSRN, Ac-PHSRN-NH_2; HSPNR, Ac-HSPNR-NH_2; bFGF, 400 μg of bFGF. *Y*-axis, mean number of microvessels per field (±SD). (B) Inhibition of PHSRN-induced angiogenesis by systemic PHSCN peptide treatment. *X*-axis, additions to Matrigel (Ac-PHSRN-NH_2, Ac-HSPNR-NH_2, or bFGF) and systemic treatments: PHSCN, Ac-PHSCN-NH_2; HSPNC, Ac-HSPNC-NH_2. *Y*-axis, mean number of microvessels per field (±SD), $n = 30$. (C) Examples of sectioned Matrigel plugs. Bars, 20 μm.

Hemoglobin Content Reduction in Matrigel Plugs with PHSRN Peptide or MATLyLu Cells

We verified that systemic PHSCN could reduce PHSRN-induced, $\alpha_5\beta_1$-mediated neovascularization in Matrigel plugs by quantitating its effects on hemoglobin content. Angiogenesis was induced by inclusion of 2.5 mg of PHSRN per plug, followed by biweekly injections of 1.25 mg of PHSRN directly into each plug. Analogous procedures were followed for the HSPNR control. After 16 days and a total of seven intravenous injections of 15 mg/kg PHSCN or HSPNC in NS (or of NS alone), the effects on PHSRN-induced angiogenesis, as indicated by hemoglobin content, were evaluated by Drabkin assay, as described [30]. As shown in Figure 8*A*, the PHSRN-induced increase in hemoglobin content of Matrigel plugs was completely prevented by systemic PHSCN, but unaffected by HSPNC, given at an identical dosage schedule.

The antiangiogenic activity of systemic PHSCN was also assessed in mice bearing Matrigel plugs, each implanted with 2 million MATLyLu rat prostate cancer cells, a commonly used model of metastatic prostate cancer [43], to induce angiogenesis. As shown in Figure 8*B*, MATLyLu cells increased the mean hemoglobin content of the Matrigel plugs by approximately three-fold after 9 days, compared with plugs containing Matrigel alone. Thrice weekly, 0.3-mg intravenous doses of PHSCN peptide prevented MATLyLu-induced angiogenesis, as indicated by reduced hemoglobin content, whereas treatment with HSPNC had no effect. These results are consistent with both the effects of systemic PHSCN peptide on angiogenesis in Matrigel plugs containing PHSRN (Figure 7*B*) and the antiangiogenic effects of systemic PHSCN therapy in rats bearing MATLyLu tumors [1].

Regulation of Cell Surface $\alpha_5\beta_1$ Integrin Levels in Endothelial Cells in Matrigel Plugs by PHSRN and PHSCN Peptides

Matrigel plugs containing various doses of the PHSRN peptide were injected into the groins of female, nude mice. After 5 days, the plugs were removed, sectioned, and stained with anti-α_5 Ab, anti-$\alpha_5\beta_1$ P1D6 mAb, or anti–MMP-1 Ab, and with DAPI. Confocal microscopy was used to quantitate immunofluorescence in the vasculature of immunostained, sectioned plugs, and the results are shown in Figure 9. Figure 9*A* shows typical examples of sectioned Matrigel plugs, containing various amounts of acetylated, amidated PHSRN peptide, ranging from 0.1 to 2.5 mg per plug. These sections were reacted with fluorescein-coupled anti-α_5 and rhodamine-coupled anti–MMP-1 Ab. Compared with plugs containing no PHSRN peptide, the endothelial cells in the microvasculature of the PHSRN-containing plugs exhibited higher levels of both anti-α_5 and anti–MMP-1 immunofluorescence, which were further increased with higher PHSRN peptide doses. Identical results were obtained with P1D6 anti-$\alpha_5\beta_1$ mAb (not shown). Mean fluorescence levels observed in 30 randomly chosen fields of five sections spanning 100 μm from duplicate Matrigel plugs were quantitated for each PHSRN concentration and control. Mean immunofluorescence levels for P1D6 anti-$\alpha_5\beta_1$ (*gray bars*), anti-α_5 Ab (*black bars*), and anti–MMP-1 Ab (*white bars*) are plotted with their first SDs. As shown in Figure 9*B*, mean surface levels of anti-$\alpha_5\beta_1$, anti-α_5, and anti–MMP-1 antibodies increased with PHSRN dose, in proportion to the increased vascularization shown in Figure 7*A*. Figure 9*C* shows typical examples of sectioned Matrigel plugs, containing 2.5 mg of PHSRN peptide, where the mice received systemic doses of PHSCN peptide in NS, ranging from 10 to 300 μg. Some mice had PHSRN-containing plugs but received only NS systemically. Sections were reacted with fluorescein-coupled anti-α_5 and rhodamine-coupled anti–MMP-1 Ab. Compared with plugs containing 2.5 mg of PHSRN peptide, in mice receiving systemic NS only, the endothelial cells in the microvasculature of the PHSRN-containing plugs from mice dosed with PHSCN peptide systemically exhibited lower levels of both anti-α_5 and anti–MMP-1 immunofluorescence and immunofluorescence decreased with higher systemic PHSCN peptide doses. Very similar results were obtained with P1D6 anti-$\alpha_5\beta_1$ mAb (not shown). Figure 9*D* shows the quantitation of the

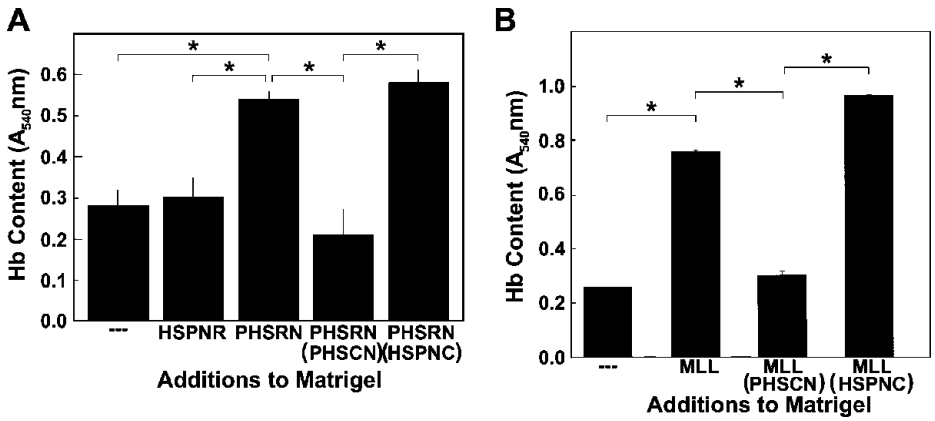

Figure 8. Inhibition of PHSRN or MATLyLu-induced angiogenesis in Matrigel plugs by systemic PHSCN: Drabkin assays. (A) Inhibition of PHSRN-induced angiogenesis in Matrigel plugs by systemic PHSCN. *X*-axis, additions to Matrigel and systemic treatments: HSPNR, 0.1 mg of Ac-HSPNR-NH_2 added to Matrigel plugs; PHSRN, 0.1 mg of Ac-PHSRN-NH_2 added to Matrigel plugs; PHSRN + PHSCN, 0.1 mg of Ac-PHSRN-NH_2 added to Matrigel plugs, with thrice weekly dosages of Ac-PHSCN-NH_2 at 15 mg/kg; PHSRN + HSPNC, 0.1 mg of Ac-PHSRN-NH_2 added to Matrigel plugs, with thrice weekly dosages of Ac-HSPNC-NH_2 at 15 mg/kg. *Y*-axis, hemoglobin (Hb) content: mean absorbance at 540 nm ($A_{540\ nm}$, ±SD). (B) Inhibition of MATLyLu-induced angiogenesis by systemic PHSCN. *X*-axis, additions to Matrigel and systemic treatments: —, Matrigel only; MLL, Matrigel + MATLyLu cells; PHSCN, 0.3 mg (15 mg/kg) of Ac-PHSCN-NH_2; HSPNC, 0.3 mg (15 mg/kg) of Ac-HSPNC-NH_2. *Y*-axis, hemoglobin (Hb) content: mean absorbance at 540 nm ($A_{540\ nm}$, ±SD). *$P < .01$.

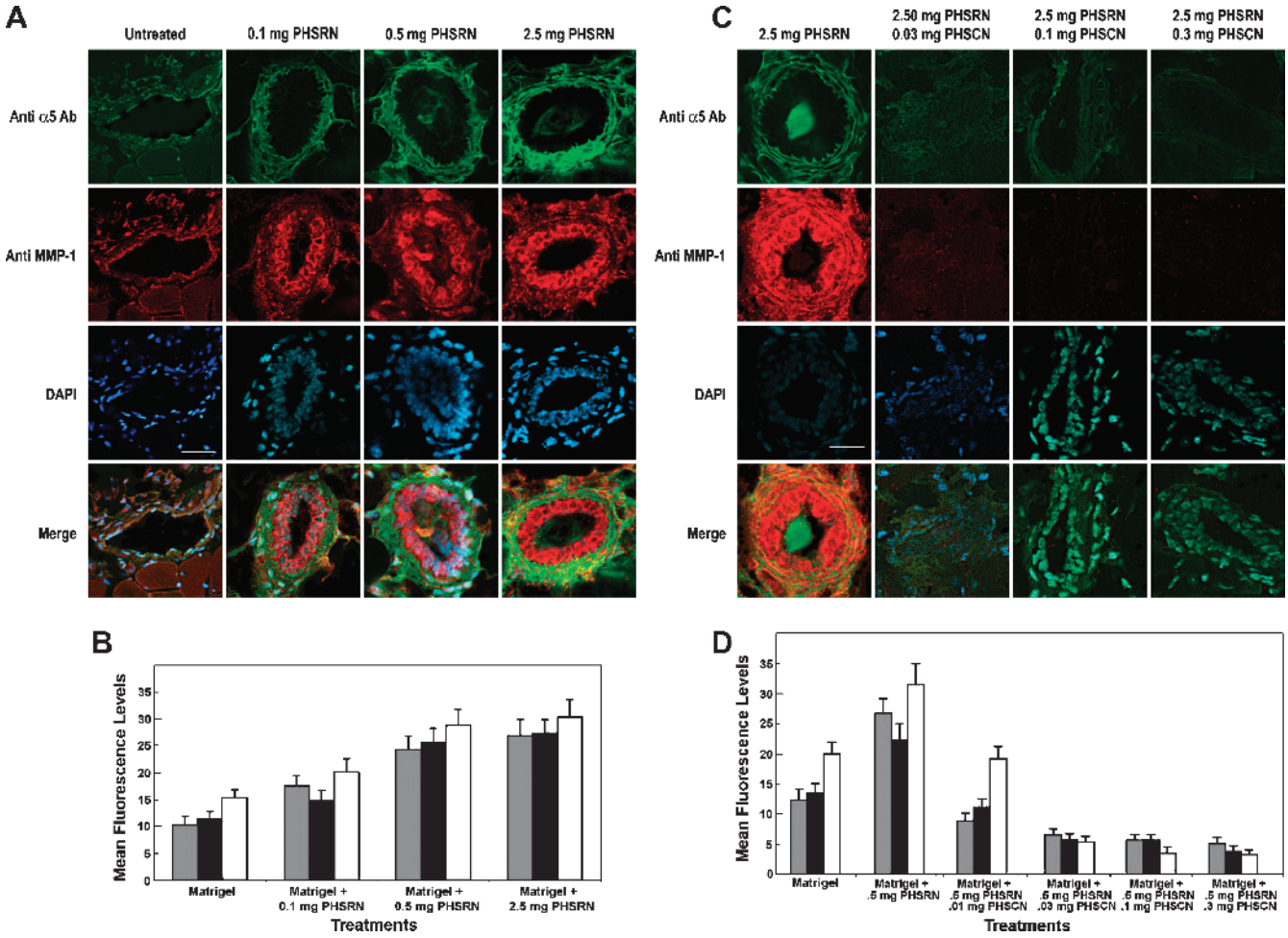

Figure 9. PHSCN inhibition of PHSRN-induced $\alpha_5\beta_1$ and MMP-1 up-regulation in Matrigel plugs. (A) Examples of sectioned PHSRN-treated Matrigel plugs stained with fluorescein-coupled anti-α_5 antiserum and rhodamine-coupled anti–MMP-1 antiserum. PHSRN doses are as shown. Bar, 20 μm. (B) Quantitation of fluorescence levels in sectioned PHSRN-treated Matrigel plugs stained with fluorescein-coupled anti-α_5 antiserum and rhodamine-coupled anti–MMP-1 antiserum. *X*-axis, peptide treatments; *Y*-axis, mean fluorescence levels (±SD). PHSRN, Ac-PHSRN-NH_2; gray bars, P1D6 mAb; black bars, anti-α_5 Ab; white bars, anti–MMP-1 Ab. (C) Examples of sectioned PHSRN-treated Matrigel plugs from mice receiving systemic PHSCN therapy at the doses shown, stained with fluorescein-coupled anti-α_5 antiserum and rhodamine-coupled anti–MMP-1 antiserum. Amount of PHSRN in all Matrigel plugs: 2.5 mg. Bar, 20 μm. Systemic PHSCN doses are as shown: 0.03, 0.1, and 0.3 mg. (D) Inhibition of PHSRN-induced $\alpha_5\beta_1$ up-regulation by systemic PHSCN peptide treatment. *X*-axis, additions to Matrigel: PHSRN, Ac-PHSRN-NH_2; PHSCN, Ac-PHSCN-NH_2. *Y*-axis, mean number of microvessels per field (±SD). Gray bars, P1D6 mAb; black bars, anti-α_5 Ab; white bars, anti–MMP-1 Ab.

mean fluorescence levels observed in 30 randomly chosen fields of five sections spanning 100 μm from duplicate Matrigel plugs for each systemic PHSCN concentration and control. Mean surface levels of fluorescent anti-$\alpha_5\beta_1$ mAb and anti-α_5 and anti–MMP-1 Ab decreased with the PHSCN dose, in proportion to the decreased vascularization shown in Figure 7*B*.

Discussion

The $\alpha_5\beta_1$ FnR plays a key role in mediating invasion by endothelial cells in the early stages of angiogenesis during embryogenesis, organogenesis, and wound healing [14,15,44–47]. Whereas $\alpha_5\beta_1$ is expressed at low levels in quiescent endothelium, surface levels of $\alpha_5\beta_1$ are greatly upregulated in activated endothelial cells and in tumor vasculature [12,16,45]. Results presented here suggest that the PHSRN peptide interacts with the $\alpha_5\beta_1$ receptors of HMVEC to induce invasion by upregulating surface $\alpha_5\beta_1$ expression through increased expression of the α_5 integrin gene. Substantial PHSRN-induced $\alpha_5\beta_1$ up-regulation was observed *in vitro* on the surfaces of adherent HMVEC and *in vivo* on the endothelial cells of the microvasculature in PHSRN-treated Matrigel plugs.

Our results also show that the PHSRN peptide ligand of $\alpha_5\beta_1$ FnR induces HMVEC invasion, similar to observations for normal human epithelial cells and neonatal fibroblasts [1–3]. PHSRN-induced, $\alpha_5\beta_1$-mediated invasion is inhibited by the $\alpha_4\beta_1$/Fn LDV interaction as observed for mammary epithelial cells [3]. Moreover, whereas blocking anti-$\alpha_5\beta_1$ mAb prevents PHSRN-induced invasion, blocking anti-$\alpha_4\beta_1$ mAb induces dose-dependent invasion and $\alpha_4\beta_1$-induced invasion specifically requires pFn. Exposure to PHSRN also stimulates MMP-1 secretion, as it does for several types of epithelial cells and fibroblasts; moreover, equimolar LDV blocks PHSRN-induced MMP-1. These results are consistent with the finding that the $\alpha_5\beta_1$/Fn CBD interaction induces MMP-1 secretion, which is blocked by the $\alpha_4\beta_1$/LDV interaction in intact Fn [37]. $\alpha_5\beta_1$-Mediated invasion specifically requires MMP-1 because both PHSRN- and anti–$\alpha_4\beta_1$-induced

HMVEC invasion are prevented dose dependently by increasing concentrations of blocking anti–MMP-1 mAb. MMP-1 is one of four MMPs that degrades native interstitial collagen, including types I, II, III, and other fibrillar collagens [48]. MMP-1 is required for angiogenesis *in vitro* [38]. It functions in endothelial cell migration through the extracellular matrix during the earliest stages of angiogenesis, perhaps by removing barriers at the leading edges of angiogenic sprouts [49,50].

Although the induction of $\alpha_5\beta_1$-meditated, MMP-1–dependent invasiveness in PHSRN-treated microvascular endothelial cells may have been expected given the role of the PHSRN/$\alpha_5\beta_1$ interaction in invasion induction by normal human fibroblasts and epithelial cells [1–4], $\alpha_5\beta_1$ up-regulation on the surfaces of PHSRN-treated HMVEC *in vitro* and in PHSRN-treated Matrigel plugs *in vivo*, the rapid induction of α_5 mRNA by PHSRN treatment, and the necessity of α_5 gene transcription for PHSRN-stimulated invasion were unanticipated consequences of the PHSRN/$\alpha_5\beta_1$ interaction. Exposure to angiogenic growth factors, such as bFGF and transforming growth factor β_1, is known to stimulate increased α_5 mRNA without inducing β_1 in microvascular endothelial cells, for example [12]; however, specific induction of α_5 mRNA as a direct result of the interaction of $\alpha_5\beta_1$ with its natural ligand, the PHSRN sequence, has not been reported previously. Our results suggest that this interaction may also play a significant role in the up-regulation of $\alpha_5\beta_1$ receptors observed on activated endothelial cells and in tumor vasculature [12,16,45] and that a feed-forward $\alpha_5\beta_1$ up-regulation in the absence of a corresponding increase in surface $\alpha_4\beta_1$ receptors may be an important mechanism for inducing endothelial cell invasion to stimulate angiogenesis. The ability of inflammatory pathways to upregulate their own ligands or receptors, thereby resulting in feed-forward signals, has been proposed to be a key feature of inflammation and tumor development, for example [51,52].

The results presented here also show that the PHSCN peptide (ATN-161), an invasion inhibitor that prevented metastatic disease progression and recurrence for prolonged periods in preclinical models and in phase 1 clinical trial [1,8–11], blocks $\alpha_5\beta_1$-mediated HMVEC invasion, whether induced by the Fn CBD, blocking anti-$\alpha_4\beta_1$ mAb, or PHSRN peptide. Furthermore, we also report that PHSCN prevents PHSRN-induced $\alpha_5\beta_1$ up-regulation and α_5 mRNA induction *in vitro* in adherent HMVEC, as expected from its ability to interact with $\alpha_5\beta_1$ to inhibit invasion induction [1,2,9–11]. Systemic PHSCN therapy was also found to inhibit $\alpha_5\beta_1$-mediated, PHSRN-induced neovascularization in Matrigel plugs. Results of microvessel scoring and Drabkin hemoglobin assays show that PHSCN therapy significantly reduces angiogenesis in Matrigel plugs, whether induced by inclusion of PHSRN peptide to directly stimulate endothelial $\alpha_5\beta_1$ receptors or metastatic MATLyLu cells [43]. We also observed that systemic PHSCN therapy downregulates surface levels of $\alpha_5\beta_1$ integrin and MMP-1 on the endothelial cells of the microvasculature in PHSRN-treated Matrigel plugs, suggesting that PHSCN may block angiogenesis *in vivo* in part through its inhibitory effects on $\alpha_5\beta_1$ up-regulation.

Because tumor vascularization promotes both tumorigenesis and metastasis, inhibition of $\alpha_5\beta_1$ may thus form the basis of potent, nontoxic antitumorigenic and antimetastatic therapies [1,6,8–11]. Angiogenesis leading to excess neovascularization contributes to several diseases, including macular degeneration [14], atherosclerosis [53], and asthma [54], as well as tumor growth and metastasis. Thus, the importance of $\alpha_5\beta_1$ integrin in angiogenesis suggests that targeted, nontoxic inhibitors of activated $\alpha_5\beta_1$ may also be useful in treating these diseases.

Acknowledgments

The authors thank Andrew Mazar (Attenuon, LLC, San Diego, CA) for informative technical consultations regarding Matrigel plug assays and for providing the PHSCN peptide (ATN-161). The authors thank Jason Gestwicki (University of Michigan, Ann Arbor, MI) for use of his laboratory's fluorescence plate reader. The authors also thank Steven Kronenberg (Department of Radiation Oncology, University of Michigan, Ann Arbor, MI) for assistance with figure preparation. A. Spalding has been designated B. Leonard Holman Pathway Fellow by the American Board of Radiology.

References

[1] Livant DL, Brabec RK, Pienta KJ, Allen DL, Kurachi K, Markwart S, and Upadhyaya A (2000). Anti-invasive, antitumorigenic, and antimetastatic activities of the PHSCN sequence in prostate carcinoma. *Cancer Res* **60**, 309–320.

[2] Livant DL, Brabec RK, Kurachi K, Allen DL, Wu Y, Haaseth R, Andrews P, Ethier SP, and Markwart S (2000). The PHSRN sequence induces extracellular matrix invasion and accelerates wound healing in obese diabetic mice. *J Clin Invest* **105**, 1537–1545.

[3] Jia Y, Zeng ZZ, Markwart SM, Rockwood KF, Ignatoski KM, Ethier SP, and Livant DL (2004). Integrin fibronectin receptors in matrix metalloproteinase-1–dependent invasion by breast cancer and mammary epithelial cells. *Cancer Res* **64**, 8674–8681.

[4] Zeng ZZ, Jia Y, Hahn NJ, Markwart SM, Rockwood KF, and Livant DL (2006). Role of focal adhesion kinase and phosphatidylinositol 3′-kinase in integrin fibronectin receptor–mediated, matrix metalloproteinase-1–dependent invasion by metastatic prostate cancer cells. *Cancer Res* **66**, 8091–8099.

[5] Garmy-Susini B, Jin H, Zhu Y, Sung RJ, Hwang R, and Varner J (2005). Integrin alpha4beta1–VCAM-1–mediated adhesion between endothelial and mural cells is required for blood vessel maturation. *J Clin Invest* **115**, 1542–1551.

[6] Livant DL (2005). Targeting invasion induction as a therapeutic strategy for the treatment of cancer. *Curr Cancer Drug Targets* **5**, 489–503.

[7] Maschler S, Wirl G, Spring H, Bredow DV, Sordat I, Beug H, and Reichmann E (2005). Tumor cell invasiveness correlates with changes in integrin expression and localization. *Oncogene* **24**, 2032–2041.

[8] Cianfrocca ME, Kimmel KA, Gallo J, Cardoso T, Brown MM, Hudes G, Lewis N, Weiner L, Lam GN, Brown SC, et al. (2006). Phase 1 trial of the antiangiogenic peptide ATN-161 (Ac-PHSCN-NH(2)), a beta integrin antagonist, in patients with solid tumours. *Br J Cancer* **94**, 1621–1626.

[9] Khalili P, Arakelian A, Chen G, Plunkett ML, Beck I, Parry GC, Donate F, Shaw DE, Mazar AP, and Rabbani SA (2006). A non–RGD-based integrin binding peptide (ATN-161) blocks breast cancer growth and metastasis *in vivo*. *Mol Cancer Ther* **5**, 2271–2280.

[10] Stoeltzing O, Liu W, Reinmuth N, Fan F, Parry GC, Parikh AA, McCarty MF, Bucana CD, Mazar AP, and Ellis LM (2003). Inhibition of integrin alpha5beta1 function with a small peptide (ATN-161) plus continuous 5-FU infusion reduces colorectal liver metastases and improves survival in mice. *Int J Cancer* **104**, 496–503.

[11] van Golen KL, Bao L, Brewer GJ, Pienta KJ, Kamradt JM, Livant DL, and Merajver SD (2002). Suppression of tumor recurrence and metastasis by a combination of the PHSCN sequence and the antiangiogenic compound tetrathiomolybdate in prostate carcinoma. *Neoplasia* **4**, 373–379.

[12] Collo G and Pepper MS (1999). Endothelial cell integrin alpha5beta1 expression is modulated by cytokines and during migration *in vitro*. *J Cell Sci* **112** (Pt 4), 569–578.

[13] Enenstein J, Waleh NS, and Kramer RH (1992). Basic FGF and TGF-beta differentially modulate integrin expression of human microvascular endothelial cells. *Exp Cell Res* **203**, 499–503.

[14] Umeda N, Kachi S, Akiyama H, Zahn G, Vossmeyer D, Stragies R, and Campochiaro PA (2006). Suppression and regression of choroidal neovascularization by systemic administration of an alpha5beta1 integrin antagonist. *Mol Pharmacol* **69**, 1820–1828.

[15] Milner R and Campbell IL (2002). Developmental regulation of beta1 integrins during angiogenesis in the central nervous system. *Mol Cell Neurosci* **20**, 616–626.

[16] Magnussen A, Kasman IM, Norberg S, Baluk P, Murray R, and McDonald DM (2005). Rapid access of antibodies to alpha5beta1 integrin overexpressed on the luminal surface of tumor blood vessels. *Cancer Res* **65**, 2712–2721.

[17] Parsons-Wingerter P, Kasman IM, Norberg S, Magnussen A, Zanivan S, Rissone A, Baluk P, Favre CJ, Jeffry U, Murray R, et al. (2005). Uniform overexpression and rapid accessibility of alpha5beta1 integrin on blood vessels in tumors. *Am J Pathol* **167**, 193–211.

[18] Livant DL, Linn S, Markwart S, and Shuster J (1995). Invasion of selectively permeable sea urchin embryo basement membranes by metastatic tumor cells, but not by their normal counterparts. *Cancer Res* **55**, 5085–5093.

[19] Vila-Carriles WH, Zhou ZH, Bubien JK, Fuller CM, and Benos DJ (2007). Participation of the chaperone Hsc70 in the trafficking and functional expression of ASIC2 in glioma cells. *J Biol Chem* **282**, 34381–34391.

[20] Zatyka M, Ricketts C, da Silva Xavier G, Minton J, Fenton S, Hofmann-Thiel S, Rutter GA, and Barrett TG (2008). Sodium-potassium ATPase 1 subunit is a molecular partner of Wolframin, an endoplasmic reticulum protein involved in ER stress. *Hum Mol Genet* **17**, 190–200.

[21] Yao H, Dashner EJ, van Golen CM, and van Golen KL (2006). RhoC GTPase is required for PC-3 prostate cancer cell invasion but not motility. *Oncogene* **25**, 2285–2296.

[22] Tashiro M, Schafer C, Yao H, Ernst SA, and Williams JA (2001). Arginine induced acute pancreatitis alters the actin cytoskeleton and increases heat shock protein expression in rat pancreatic acinar cells. *Gut* **49**, 241–250.

[23] Tsunoda Y, Yao H, Park J, and Owyang C (2003). Cholecystokinin synthesizes and secretes leptin in isolated canine gastric chief cells. *Biochem Biophys Res Commun* **310**, 681–684.

[24] Anderson JA, Grabowska AM, and Watson SA (2007). PTHrP increases transcriptional activity of the integrin subunit alpha5. *Br J Cancer* **96**, 1394–1403.

[25] Oki N, Matsuo H, Nakago S, Murakoshi H, Laoag-Fernandez JB, and Maruo T (2004). Effects of 3,5,3′-triiodothyronine on the invasive potential and the expression of integrins and matrix metalloproteinases in cultured early placental extravillous trophoblasts. *J Clin Endocrinol Metab* **89**, 5213–5221.

[26] Albertin G, Ruggero M, Guidolin D, and Nussdorfer GG (2006). Gene silencing of human RAMP2 mediated by short-interfering RNA. *Int J Mol Med* **18**, 531–535.

[27] Han S, Ritzenthaler JD, Sitaraman SV, and Roman J (2006). Fibronectin increases matrix metalloproteinase 9 expression through activation of c-Fos via extracellular-regulated kinase and phosphatidylinositol 3-kinase pathways in human lung carcinoma cells. *J Biol Chem* **281**, 29614–29624.

[28] Wang GK, Hu L, Fuller GN, and Zhang W (2006). An interaction between insulin-like growth factor–binding protein 2 (IGFBP2) and integrin alpha5 is essential for IGFBP2-induced cell mobility. *J Biol Chem* **281**, 14085–14091.

[29] Albig AR, Neil JR, and Schiemann WP (2006). Fibulins 3 and 5 antagonize tumor angiogenesis *in vivo*. *Cancer Res* **66**, 2621–2629.

[30] Donate F, Juarez JC, Guan X, Shipulina NV, Plunkett ML, Tel-Tsur Z, Shaw DE, Morgan WT, and Mazar AP (2004). Peptides derived from the histidine-proline domain of the histidine-proline–rich glycoprotein bind to tropomyosin and have antiangiogenic and antitumor activities. *Cancer Res* **64**, 5812–5817.

[31] Malinda KM (2003). *In vivo* Matrigel migration and angiogenesis assays. *Methods Mol Med* **78**, 329–335.

[32] Altroff H, van der Walle CF, Asselin J, Fairless R, Campbell ID, and Mardon HJ (2001). The eighth FIII domain of human fibronectin promotes integrin alpha5beta1 binding via stabilization of the ninth FIII domain. *J Biol Chem* **276**, 38885–38892.

[33] Aota S, Nomizu M, and Yamada KM (1994). The short amino acid sequence Pro-His-Ser-Arg-Asn in human fibronectin enhances cell-adhesive function. *J Biol Chem* **269**, 24756–24761.

[34] Komoriya A, Green LJ, Mervic M, Yamada SS, Yamada KM, and Humphries MJ (1991). The minimal essential sequence for a major cell type–specific adhesion site (CS1) within the alternatively spliced type III connecting segment domain of fibronectin is leucine–aspartic acid–valine. *J Biol Chem* **266**, 15075–15079.

[35] Mettouchi A and Meneguzzi G (2006). Distinct roles of beta1 integrins during angiogenesis. *Eur J Cell Biol* **85**, 243–247.

[36] Wayner EA, Carter WG, Piotrowicz RS, and Kunicki TJ (1988). The function of multiple extracellular matrix receptors in mediating cell adhesion to extracellular matrix: preparation of monoclonal antibodies to the fibronectin receptor that specifically inhibit cell adhesion to fibronectin and react with platelet glycoproteins Ic-IIa. *J Cell Biol* **107**, 1881–1891.

[37] Huhtala P, Humphries MJ, McCarthy JB, Tremble PM, Werb Z, and Damsky CH (1995). Cooperative signaling by alpha 5 beta 1 and alpha 4 beta 1 integrins regulates metalloproteinase gene expression in fibroblasts adhering to fibronectin. *J Cell Biol* **129**, 867–879.

[38] Fisher C, Gilbertson-Beadling S, Powers EA, Petzold G, Poorman R, and Mitchell MA (1994). Interstitial collagenase is required for angiogenesis *in vitro*. *Dev Biol* **162**, 499–510.

[39] Tian Q, Stepaniants SB, Mao M, Weng L, Feetham MC, Doyle MJ, Yi EC, Dai H, Thorsson V, Eng J, et al. (2004). Integrated genomic and proteomic analyses of gene expression in Mammalian cells. *Mol Cell Proteomics* **3**, 960–969.

[40] Akhtar N, Dickerson EB, and Auerbach R (2002). The sponge/Matrigel angiogenesis assay. *Angiogenesis* **5**, 75–80.

[41] Kibbey MC, Grant DS, and Kleinman HK (1992). Role of the SIKVAV site of laminin in promotion of angiogenesis and tumor growth: an *in vivo* Matrigel model. *J Natl Cancer Inst* **84**, 1633–1638.

[42] Donate F, Parry GC, Shaked Y, Hensley H, Guan X, Beck I, Tel-Tsur Z, Plunkett ML, Manuia M, Shaw DE, et al. (2008). Pharmacology of the novel antiangiogenic peptide ATN-161 (Ac-PHSCN-NH_2): observation of a U-shaped dose-response curve in several preclinical models of angiogenesis and tumor growth. *Clin Cancer Res* **14**, 2137–2144.

[43] Isaacs JT, Isaacs WB, Feitz WF, and Scheres J (1986). Establishment and characterization of seven Dunning rat prostatic cancer cell lines and their use in developing methods for predicting metastatic abilities of prostatic cancers. *Prostate* **9**, 261–281.

[44] Francis SE, Goh KL, Hodivala-Dilke K, Bader BL, Stark M, Davidson D, and Hynes RO (2002). Central roles of alpha5beta1 integrin and fibronectin in vascular development in mouse embryos and embryoid bodies. *Arterioscler Thromb Vasc Biol* **22**, 927–933.

[45] Kim S, Bell K, Mousa SA, and Varner JA (2000). Regulation of angiogenesis *in vivo* by ligation of integrin alpha5beta1 with the central cell-binding domain of fibronectin. *Am J Pathol* **156**, 1345–1362.

[46] Kloss CU, Werner A, Klein MA, Shen J, Menuz K, Probst JC, Kreutzberg GW, and Raivich G (1999). Integrin family of cell adhesion molecules in the injured brain: regulation and cellular localization in the normal and regenerating mouse facial motor nucleus. *J Comp Neurol* **411**, 162–178.

[47] Roman J and McDonald JA (1992). Expression of fibronectin, the integrin alpha 5, and alpha-smooth muscle actin in heart and lung development. *Am J Respir Cell Mol Biol* **6**, 472–480.

[48] Lee MH and Murphy G (2004). Matrix metalloproteinases at a glance. *J Cell Sci* **117** (Pt 18), 4015–4016.

[49] Partridge CR, Hawker JR Jr, and Forough R (2000). Overexpression of a secretory form of FGF-1 promotes MMP-1–mediated endothelial cell migration. *J Cell Biochem* **78**, 487–499.

[50] Unemori EN, Ferrara N, Bauer EA, and Amento EP (1992). Vascular endothelial growth factor induces interstitial collagenase expression in human endothelial cells. *J Cell Physiol* **153**, 557–562.

[51] Dougan M and Dranoff G (2008). Inciting inflammation: the RAGE about tumor promotion. *J Exp Med* **205**, 267–270.

[52] Gebhardt C, Riehl A, Durchdewald M, Nemeth J, Furstenberger G, Muller-Decker K, Enk A, Arnold B, Bierhaus A, Nawroth PP, et al. (2008). RAGE signaling sustains inflammation and promotes tumor development. *J Exp Med* **205**, 275–285.

[53] Kolodgie FD, Narula J, Yuan C, Burke AP, Finn AV, and Virmani R (2007). Elimination of neoangiogenesis for plaque stabilization: is there a role for local drug therapy? *J Am Coll Cardiol* **49**, 2093–2101.

[54] Asosingh K, Swaidani S, Aronica M, and Erzurum SC (2007). T_H1- and T_H2-dependent endothelial progenitor cell recruitment and angiogenic switch in asthma. *J Immunol* **178**, 6482–6494.